

Orientations of a Nematic Liquid Crystal in Sandwich-Type Cells Studied by Polarized Electronic Absorption Spectra

Michio KOBAYASHI,* Yoshinori KATO, Norio KOMA, Naobumi TAKI,
Kazunori MARUYAMA, and Yoshie TANIZAKI

Department of Chemistry, Nagaoka University of Technology,
Kamitomioka-machi, Nagaoka 940-21

(Received June 6, 1992)

Polarized electronic absorption spectra of a nematic liquid crystal (4-butyl-4'-ethoxyazobenzene, BEAB) were measured in sandwich-type cells to which no rubbing treatment was applied. These polarized spectra were utilized to evaluate the mean squares of the direction cosines of the transition moment, those of the molecular orientation axis, and the three-dimensional absorption components as a function of the cell gap. It has been shown that the inclinations of the transition moment for the 354 nm band (long-axis polarized) and the molecular orientation axis to the cell plane increase with the decrease in the cell gap while the absorption component for the 354 nm band normal to the cell plane decreases. These observations provide a quantitative support for the molecular orientation model proposed previously that the molecular long axis tends to be oriented parallel to the cell plane in the interface region and perpendicular in the bulk region. The thickness of the interface region has been estimated to be about 0.02 μm by a model calculation based on a discrete model for the orientation of the BEAB molecules in the cell.

Nematic liquid crystals can be oriented by rubbing, magnetic field, and flow.¹⁾ The order parameters²⁾ of oriented liquid crystals have been estimated by utilizing optical properties associated with the refractive index or by utilizing spectroscopic and magnetic anisotropies of guest molecules in the host of oriented liquid crystals.³⁾ Anisotropic absorption spectra of oriented liquid crystals themselves have rarely been measured to estimate their order parameters except few cases.^{4,5)} We previously measured the absorption spectra of a nematic liquid-crystalline (LC) molecule (4-butyl-4'-ethoxyazobenzene, BEAB) in sandwich-type cells with very thin gaps by using unpolarized light.⁶⁾ By a qualitative analysis of the intensity ratios of the 354 nm band (long-axis polarized) to the 240 nm band (short-axis polarized) for the (bulk+interface) spectra with various gaps and those for the bulk spectra with various bulk thicknesses, we proposed a molecular orientation model for the LC molecules in a sandwich-type cell: The molecular long axis tends to be oriented parallel to the cell plane in the interface region and perpendicular in the bulk region.⁶⁾ The molecular orientation in the interface region was supposed to be induced by a weak rubbing effect via the fluid.

As pointed out briefly in our previous paper, BEAB in the LC phase exhibited a positive dichroism in a sandwich-type cell, to which no rubbing treatment was applied, the optical axis being the sucking-up direction of the melted sample into the cell.⁶⁾ In order to get more insight into the molecular orientation model mentioned above, we have measured in the present study polarized absorption spectra of BEAB in sandwich-type cells with various gaps by using polarized light. Quantitative analyses of the three-dimensional orientations of the LC molecules in the sandwich-type cells have been made, and the thickness of the interface region has been estimated by a model calculation.

Theoretical

In order to analyze the three-dimensional orientations of the LC molecules in a sandwich-type cell, equations are derived to express the direction cosines of the transition moment (μ) and the molecular orientation axis (OA)⁷⁾ in terms of the observed spectral data. In addition, a calculational procedure is given to estimate the thickness of the interface region in the sandwich-type cell by considering a discrete model for the orientation of the LC molecules in the cell.

Direction Cosines of the Transition Moment. The x , y , and z coordinate-axes for the sandwich-type cell are defined in Fig. 1. The origin of this coordinate system

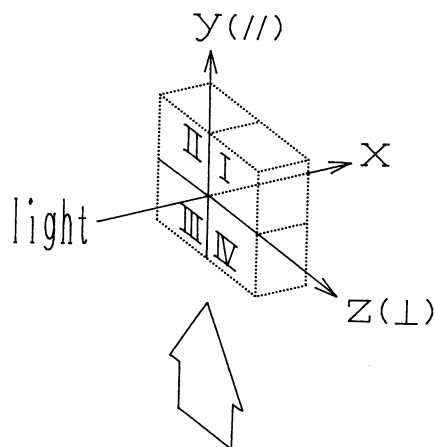


Fig. 1. Coordinate-axes defined for the sandwich-type cell; the x axis: the direction of light propagation normal to the cell plane; the $y(//)$ axis: the direction of sucking-up of melted BEAB into the cell as indicated by the arrow illustrated below the cell. The polarized absorption spectra ($A_{||}$ and A_{\perp}) of BEAB in the cell were measured by using the polarized lights whose electric vectors coincided approximately with the $y(//)$ and $z(\perp)$ axes.

need not be fixed and can be considered to coincide in position with any LC molecule in the cell. If the direction cosines of μ with respect to the x , y , and z axes are denoted by l , m , and n , respectively, the x , y , and z components of the absorption (A_x , A_y , and A_z) are given by use of the mean squares of the direction cosines of μ ($\langle l^2 \rangle$, $\langle m^2 \rangle$, and $\langle n^2 \rangle$) averaged over all the LC molecules in the cell as

$$\begin{aligned} A_x &= k\mu^2 \langle l^2 \rangle; A_y = A_z = k\mu^2 \langle m^2 \rangle; \\ A_z &= A_{\perp} = k\mu^2 \langle n^2 \rangle; \end{aligned} \quad (1)$$

and

$$A_x + A_y + A_z = k\mu^2 = 3A_{\text{iso}}; \quad (2)$$

where k is a constant and A_{iso} stands for the absorbance in the isotropic phase measured by polarized light. The second equality in Eq. 2 follows from that the polarized light is effectively absorbed by one third of the total LC molecules in the isotropic phase. These equations can be used to evaluate $\langle l^2 \rangle$, $\langle m^2 \rangle$, and $\langle n^2 \rangle$ from the observed spectral data (A_{\parallel} , A_{\perp} , and A_{iso}) for the LC molecule in the cell as

$$\begin{aligned} \langle l^2 \rangle &= 1 - (A_{\parallel} + A_{\perp})/3A_{\text{iso}}; \langle m^2 \rangle = A_{\parallel}/3A_{\text{iso}}; \\ \langle n^2 \rangle &= A_{\perp}/3A_{\text{iso}}. \end{aligned} \quad (3)$$

The angle ϕ made by the two transition moments μ_1 and μ_2 for the two bands of the LC molecule can be estimated experimentally if the root mean squares of their direction cosines ($\langle l_1^2 \rangle^{1/2}$ etc. and $\langle l_2^2 \rangle^{1/2}$ etc.) are evaluated by the use of Eq. 3. The transition moment μ_1 or μ_2 points toward any one of quadrants I, II, III, and IV in the coordinate system, whose origin coincides in position with the LC molecule, shown in Fig. 1. Without the loss of generality, μ_1 can be assumed to point toward quadrant I making $\langle l_1 \rangle$, $\langle m_1 \rangle$, and $\langle n_1 \rangle$ all positive and μ_2 toward any one of the quadrants making $\langle l_2 \rangle$ positive. If the ϕ values are defined as ϕ^I , ϕ^{II} , ϕ^{III} , and ϕ^{IV} when μ_2 points toward quadrants I, II, III, and IV, respectively, they are evaluated as

$$\phi^I = \cos^{-1}(\langle l_1^2 \rangle^{1/2} \cdot \langle l_2^2 \rangle^{1/2} + \langle m_1^2 \rangle^{1/2} \cdot \langle m_2^2 \rangle^{1/2} + \langle n_1^2 \rangle^{1/2} \cdot \langle n_2^2 \rangle^{1/2}); \quad (4-1)$$

$$\phi^{II} = \cos^{-1}(\langle l_1^2 \rangle^{1/2} \cdot \langle l_2^2 \rangle^{1/2} + \langle m_1^2 \rangle^{1/2} \cdot \langle m_2^2 \rangle^{1/2} - \langle n_1^2 \rangle^{1/2} \cdot \langle n_2^2 \rangle^{1/2}); \quad (4-2)$$

$$\phi^{III} = \cos^{-1}(\langle l_1^2 \rangle^{1/2} \cdot \langle l_2^2 \rangle^{1/2} - \langle m_1^2 \rangle^{1/2} \cdot \langle m_2^2 \rangle^{1/2} - \langle n_1^2 \rangle^{1/2} \cdot \langle n_2^2 \rangle^{1/2}); \quad (4-3)$$

$$\phi^{IV} = \cos^{-1}(\langle l_1^2 \rangle^{1/2} \cdot \langle l_2^2 \rangle^{1/2} - \langle m_1^2 \rangle^{1/2} \cdot \langle m_2^2 \rangle^{1/2} + \langle n_1^2 \rangle^{1/2} \cdot \langle n_2^2 \rangle^{1/2}). \quad (4-4)$$

Equations 3 and 4 are applicable to the molecules

oriented in a uniaxially-stretched film with some modifications. Since the molecules are oriented uniaxially in the film, it follows that

$$A_x = A_z = A_{\perp}; 3A_{\text{iso}} = A_{\parallel} + 2A_{\perp}, \quad (5)$$

where A_{\parallel} and A_{\perp} are the absorbances measured by the polarized lights whose electric vectors are parallel and perpendicular to the stretching direction of the film, respectively. Thus, Eqs. 3 and 4 are modified as follows.

$$\begin{aligned} \langle l^2 \rangle &= \langle n^2 \rangle = A_{\perp}/(A_{\parallel} + 2A_{\perp}); \\ \langle m^2 \rangle &= A_{\parallel}/(A_{\parallel} + 2A_{\perp}). \end{aligned} \quad (3')$$

$$\begin{aligned} \phi^I &= \cos^{-1}(2\langle n_1^2 \rangle^{1/2} \cdot \langle n_2^2 \rangle^{1/2} \\ &\quad + \langle m_1^2 \rangle^{1/2} \cdot \langle m_2^2 \rangle^{1/2}); \end{aligned} \quad (4'-1)$$

$$\phi^{II} = \cos^{-1}(\langle m_1^2 \rangle^{1/2} \cdot \langle m_2^2 \rangle^{1/2}); \quad (4'-2)$$

$$\phi^{III} = \cos^{-1}(-\langle m_1^2 \rangle^{1/2} \cdot \langle m_2^2 \rangle^{1/2}); \quad (4'-3)$$

$$\begin{aligned} \phi^{IV} &= \cos^{-1}(2\langle n_1^2 \rangle^{1/2} \cdot \langle n_2^2 \rangle^{1/2} \\ &\quad - \langle m_1^2 \rangle^{1/2} \cdot \langle m_2^2 \rangle^{1/2}). \end{aligned} \quad (4'-4)$$

Direction Cosines of the Molecular Orientation Axis.

The direction cosines of OA with respect of the x , y , and z axes are denoted by l' , m' , and n' , respectively. If μ makes an angle θ with OA, A_x , A_{\parallel} , and A_{\perp} are given as follows by using the mean squares of the direction cosines of OA ($\langle l'^2 \rangle$, $\langle m'^2 \rangle$, and $\langle n'^2 \rangle$) averaged over all the LC molecules in the sandwich-type cell.

$$A_x = k\mu^2[\langle l'^2 \rangle \cos^2\theta + 0.5(1 - \langle l'^2 \rangle) \sin^2\theta]; \quad (6-1)$$

$$A_{\parallel} = k\mu^2[\langle m'^2 \rangle \cos^2\theta + 0.5(1 - \langle m'^2 \rangle) \sin^2\theta]; \quad (6-2)$$

$$A_{\perp} = k\mu^2[\langle n'^2 \rangle \cos^2\theta + 0.5(1 - \langle n'^2 \rangle) \sin^2\theta]. \quad (6-3)$$

From these relations and Eq. 2, the following equations are derived:

$$\langle l'^2 \rangle = [3A_{\text{iso}}(1 - 0.5\sin^2\theta) - A_{\parallel} - A_{\perp}] / [3A_{\text{iso}}(1 - 1.5\sin^2\theta)]; \quad (7-1)$$

$$\langle m'^2 \rangle = (A_{\parallel} - 1.5\sin^2\theta A_{\text{iso}}) / [3A_{\text{iso}}(1 - 1.5\sin^2\theta)]; \quad (7-2)$$

$$\langle n'^2 \rangle = (A_{\perp} - 1.5\sin^2\theta A_{\text{iso}}) / [3A_{\text{iso}}(1 - 1.5\sin^2\theta)]. \quad (7-3)$$

Thus, since θ is evaluated as the orientation angle by Tanizaki's method for the analysis of the linear dichroism (A_{\parallel} and A_{\perp}) measured by the uniaxially-stretched film technique,⁷⁾ $\langle l'^2 \rangle$, $\langle m'^2 \rangle$, and $\langle n'^2 \rangle$ can be evaluated from the spectral data (A_{\parallel} , A_{\perp} , and A_{iso}) observed for the LC molecule in the cell.

Thickness of the Interface Region. To estimate the thickness of the interface region in the sandwich-type cell,

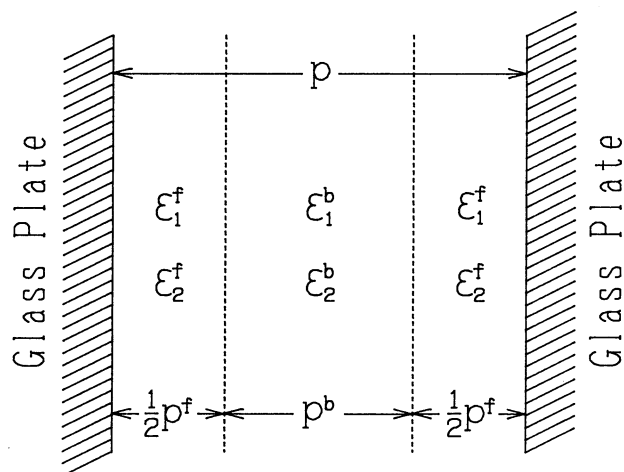


Fig. 2. A discrete model: molar absorptivities (ϵ^f , ϵ^b) and optical path lengths (p^f and p^b) in the interface and bulk regions of the sandwich-type cell.

we take a discrete model for the orientation of the LC molecules in the cell. As described in our previous paper, it is assumed in this model that there are interface and bulk regions in the cell with a distinct boundary between them and that the LC molecules are oriented homogeneously with a definite inclination in each region.⁶⁾ The interface and bulk regions exhibit their own molar absorptivities for the light. As shown in Fig. 2, ϵ_1^f and ϵ_1^b stand for the molar absorptivities for the first band of the LC molecule in the interface and bulk regions, respectively, and p^f and p^b denote their optical path lengths in the cell gap p . Thus, the intensity ratio (R_{12}) of the first and second bands of the LC molecule in the cell is expressed as

$$R_{12} = A_1/A_2 = (\epsilon_1^b p^b + \epsilon_1^f p^f) / (\epsilon_2^b p^b + \epsilon_2^f p^f) \\ = [(\epsilon_1^b/\epsilon_2^b)p^b + (\epsilon_1^f/\epsilon_2^b)p^f] / [p^b + (\epsilon_2^f/\epsilon_2^b)p^f].$$

By substitution of the relations $\epsilon_1^b/\epsilon_2^b = r_{12}^b$ and $p^b = p - p^f$, it is shown that

$$R_{12} = [r_{12}^b p - (r_{12}^b - \epsilon_1^f/\epsilon_2^b)p^f] / [p - (1 - \epsilon_2^f/\epsilon_2^b)p^f]. \quad (8)$$

Since the intensity ratio in the bulk region r_{12}^b is an experimentally-known quantity, which is invariant for all the sandwich-type cells as demonstrated in our previous paper,⁶⁾ and R_{12} and p are also known, there are formally four unknowns (ϵ_1^f , ϵ_2^f , ϵ_2^b , and p^f) in Eq. 8. For our aim to know p^f , however, it is only necessary to know $\epsilon_1^f/\epsilon_2^f$ ($=r_{12}^f$) instead of ϵ_1^f and ϵ_2^f separately. Since r_{12}^f can be obtained by taking the ratio of $\epsilon_1^f/\epsilon_2^b$ to $\epsilon_2^f/\epsilon_2^b$, there remain three unknowns ($\epsilon_1^f/\epsilon_2^b$, $\epsilon_2^f/\epsilon_2^b$, and p^f) in Eq. 8.

Assuming that p^f is invariant for all the sandwich-type cells, p^f is evaluated by solving the simultaneous equations, which arise from Eq. 8 by substitution of the R_{12} , p , and r_{12}^b values observed for various cells, under

the experimentally found constraint on r_{12}^f that r_{12}^f is larger than the R_{12} value for the isotropic phase, 1.69.⁶⁾

Experimental

Commercially available BEAB was purified by repeated recrystallization from aqueous ethanol. Sandwich-type cells of BEAB were prepared by the procedure described previously.⁶⁾ Polarized absorption spectra ($A_{||}$ and A_{\perp}) of BEAB in the cells were measured on a Shimadzu UV-360 spectrophotometer equipped with a Rochon-type polarizer, the polarized light beam entering normal to the cell plane; $A_{||}$ was defined as the polarized spectrum showing the maximum absorbance at the peak of the 354 nm band (long-axis polarized) and A_{\perp} as that showing the minimum absorbance. The direction of the electric vector of the polarized light giving $A_{||}$ coincided approximately with the direction of sucking-up of melted BEAB into the cell and was perpendicular to that of the polarized light giving A_{\perp} . The gap of the sandwich-type cell of BEAB was measured by the absorbance for the first band of BEAB in the isotropic phase as described previously.⁶⁾ The gaps of the empty cells were estimated to be in the range 0.08—0.7 μm from the interference spectra.

Results and Discussion

Figure 3 shows the polarized absorption spectra ($A_{||}$ and A_{\perp}) of BEAB in a sandwich-type cell measured in the LC phase at 70°C. $A_{||}$ was larger than A_{\perp} in the whole spectral region, demonstrating that dichroism was observed for BEAB in the cell even without the rubbing treatment on the surface of the glass plate. This dichroism disappeared when the sample cell was heated to the isotropic liquid phase, but it reappeared when cooled to the LC phase again. As discussed in our previous paper, the dichroism shown in Fig. 3 is considered to be induced by a kind of rubbing effect which is generated on the surface of the glass plate by the friction when the melted sample is sucked up into the cell.⁶⁾ By the use of the data of $A_{||}$ and A_{\perp} for BEAB in the cells with various gaps, we have analyzed the three-

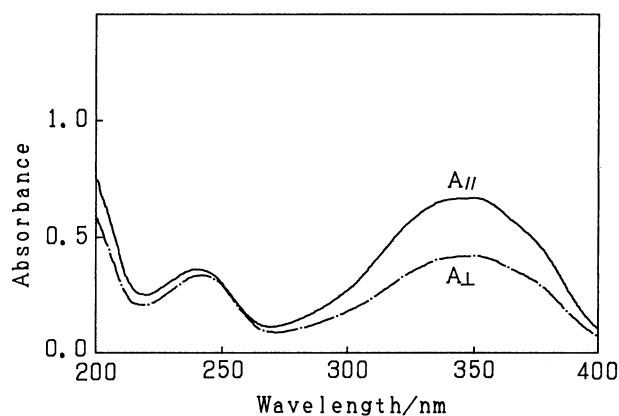


Fig. 3. Polarized absorption spectra of BEAB in the sandwich-type cell to which no rubbing treatment was applied.

dimensional orientations of the BEAB molecules in the cell and estimated the thickness of the interface region as follows.

Quantitative Analyses of the Orientations of the BEAB Molecules in the Sandwich-Type Cells. A simple way for a quantitative analysis of the three-dimensional orientations of the long axes of the BEAB molecules in the sandwich-type cell is to plot the A_x , A_y , and A_z values of the first (354 nm) band polarized along the molecular long axis⁶⁾ against the cell gap as shown in Fig. 4a; the A_x value is not measurable experimentally but can be evaluated from Eq. 2 as $A_x = 3A_{\text{iso}} - A_y - A_z = 3A_{\text{iso}} - A_{\parallel} - A_{\perp}$. In Fig. 4b, the absorbance ratios of A_x , A_y , and A_z to A_{iso} are plotted against the cell gap in order to show the cell-gap dependence of A_x , A_y , and A_z more clearly. In these figures, the plot positioned above or below the dotted line represents $A_{x,y,z}$ larger or smaller than A_{iso} . It is evident from Fig. 4b that A_x increases with the increase in the cell gap, while $A_y(A_{\parallel})$ and $A_z(A_{\perp})$ decrease, A_y being larger than A_z at all the cell gaps, and that A_y and A_x are larger than A_{iso} at smaller and larger cell gaps, respectively. These observations indicate that the transition moment of the first band, i.e. the molecular long axis, projected on the xy - or xz -plane is inclined

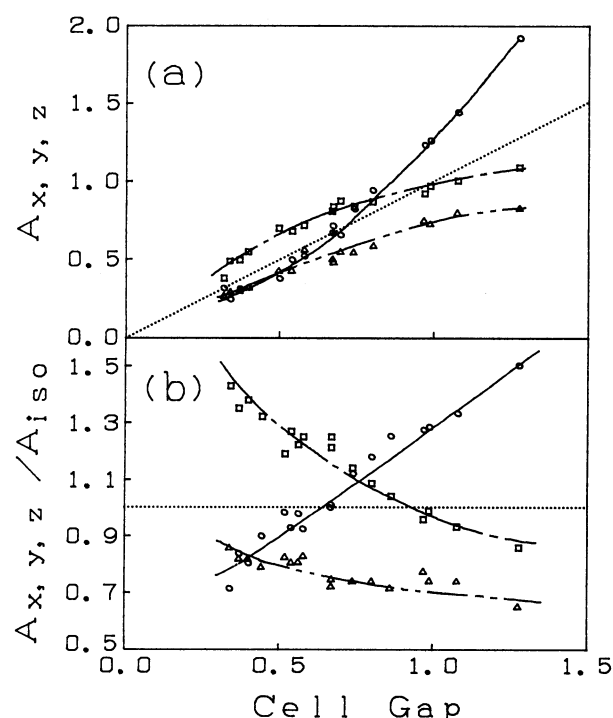


Fig. 4. Cell-gap dependences of (a) the x , y , and z absorption components (A_x , A_y , and A_z) for the first (354 nm) band of BEAB in the cell and (b) the absorbance ratios of A_x , A_y , and A_z to A_{iso} ; \circ —: (a) A_x , and (b) A_x/A_{iso} ; \square —: (a) A_y and (b) A_y/A_{iso} ; \triangle —: (a) A_z and (b) A_z/A_{iso} . A_{iso} is the absorbance for the first band of BEAB in the isotropic phase. The cell gap is graduated by A_{iso} .

Table 1. The ϕ^I , ϕ^{II} , ϕ^{III} , and ϕ^{IV} Values^{a)} Evaluated for BEAB in the Uniaxially-Stretched Film (a) and in the Sandwich-Type Cell (b)

	ϕ^I deg.	ϕ^{II} deg.	ϕ^{III} deg.	ϕ^{IV} deg.
(a) ^{b)}	15	60	120	93
(b) ^{c)}	12	61	99	70

a) See the text for their definitions. b) Evaluated from Eqs. 3' and 4' using the spectral data (A_{\parallel} and A_{\perp}) for BEAB in the uniaxially-stretched film. c) Evaluated from Eqs. 3 and 4 using the spectral data (A_{\parallel} , A_{\perp} , and A_{iso}) for the bulk spectra of BEAB in the sandwich-type cell, i.e., for the difference spectra between the spectra of BEAB in the sandwich-type cells with different gaps.

parallel to the cell plane (yz -plane) in the interface region and perpendicular in the bulk region, and the molecular long axis projected on the yz -plane is inclined rather parallel to the sucking-up ($y(\parallel)$) direction of melted BEAB into the cell both in the interface and bulk regions. Consequently, our previous model⁶⁾ for the orientation of the LC molecules in the cell is supported and refined by the cell-gap dependences of the three-dimensional absorption components shown in Fig. 4.

In order to analyze the molecular orientation three-dimensionally following the formulations presented in the Theoretical section, we have first determined the quadrant toward which the transition moment of the second (240 nm) band μ_2 points when that of the first (354 nm) band μ_1 is assumed to point toward quadrant I. In Table 1(a) are given the ϕ^I , ϕ^{II} , ϕ^{III} , and ϕ^{IV} values evaluated from Eqs. 3' and 4' using A_{\parallel} and A_{\perp} for BEAB in the uniaxially-stretched film, and in Table 1(b) those evaluated from Eqs. 3 and 4 using A_{\parallel} , A_{\perp} , and A_{iso} for BEAB in the sandwich-type cell. According to Tanizaki's method of the linear-dichroism analysis for BEAB in the uniaxially-stretched film, ϕ was evaluated as 66° .⁶⁾ This ϕ value is best reproduced in Table 1 by ϕ^{II} , i.e., when μ_2 points toward quadrant II. Thus, μ_1 and μ_2 are considered to point toward quadrants I and II, respectively, in the following discussion. In Fig. 5 we visualize the variation in the three-dimensional orientations of μ_1 and μ_2 with a change in the cell gap, the angles of μ_1 and μ_2 from the x , y , and z axes being obtained from the $\langle l_1^2 \rangle$, $\langle m_1^2 \rangle$, $\langle n_1^2 \rangle$ and $\langle l_2^2 \rangle$, $\langle m_2^2 \rangle$, $\langle n_2^2 \rangle$ values evaluated for the first and second bands using Eq. 3, respectively. The results for the bulk in this figure were obtained from an application of Eq. 3 to the difference spectra between the polarized absorption spectra of BEAB in the cells with different gaps. The axes in Fig. 5 are identical to those in Fig. 1. The cell-gap dependences and relative magnitudes of the x , $y(\parallel)$, and $z(\perp)$ components of μ_1 shown in Fig. 5 are in harmony with those of A_x , $A_y(A_{\parallel})$, and $A_z(A_{\perp})$ shown in Fig. 4a. (The results for the bulk may be regarded as those for the cell with an infinite gap). Therefore, Fig. 5

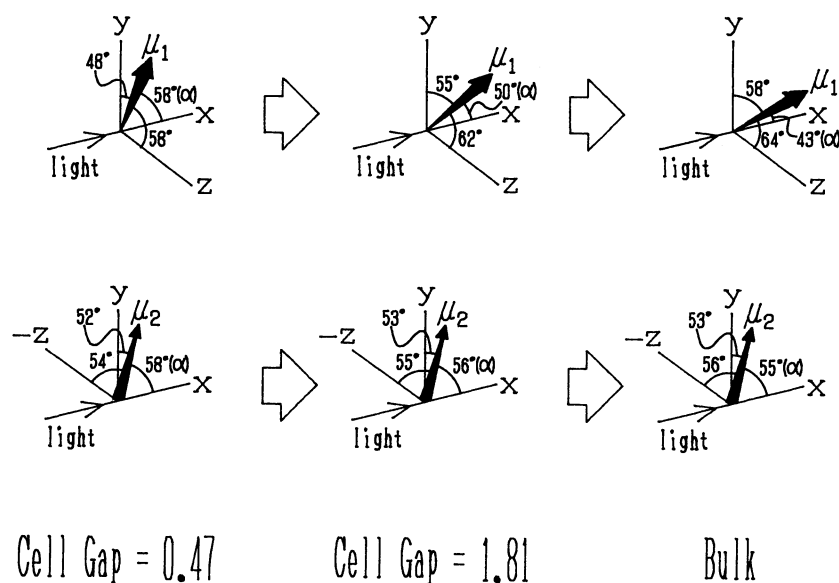


Fig. 5. Variations in the orientations of the transition moments for the first (354 nm) and second (240 nm) bands of BEAB (μ_1 and μ_2) with a change in the cell gap. The cell gaps given are the absorbance for the first band of BEAB in the isotropic phase. The bulk is regarded as an infinite cell-gap.

gives the same orientational distribution of the molecular long axis, along which μ_1 points,⁶⁾ of BEAB in the cell as that indicated by Fig. 4b. A remarkable feature of Fig. 5 is that the angle α made by μ_1 with the x -axis increases with the decrease in the cell gap, whereas the orientation of μ_2 is independent of the cell gap. (It should be noted that the directions of μ_1 and μ_2 in Fig. 5 result from a vector sum for many BEAB molecules, which are oriented differently in the interface and bulk regions of the cell, and hence the mean angle between μ_1 and μ_2 can vary with the cell gap, as seen in Fig. 5.) This observation implies that μ_1 , i.e. the molecular long axis of BEAB, is inclined to the cell plane (yz -plane) to a larger extent as the proportion of the interface region to the bulk region is increased. Thus, our previous model⁶⁾ for the orientation of the LC molecules in the cell is supported and refined.

Since OA approximately coincides with the molecular long axis, the inclination of the molecular long axis of BEAB to the cell plane can also be estimated from the mean square of the direction cosine of OA with respect to the x -axis ($\langle l'^2 \rangle$) averaged over all the BEAB molecules in the cell. The $\langle l'^2 \rangle$ values have been calculated from Eq. 7-1 by using the data for the first band, i.e., the θ value ($=17.5^\circ$; see Table 1 in Ref. 6) and the spectral data ($A_{||}$, A_{\perp} , and A_{iso}) observed for the cells with various gaps. The $\langle l'^2 \rangle$ values thus calculated are plotted against the cell gaps in Fig. 6, where the mean angles $\langle \beta \rangle$ made by OA and the cell plane, evaluated from the relation $\langle l'^2 \rangle = \sin^2 \langle \beta \rangle$, are also given. This figure shows that OA, i.e. the molecular long axis of BEAB, is inclined to the cell plane to a larger extent as the cell gap becomes

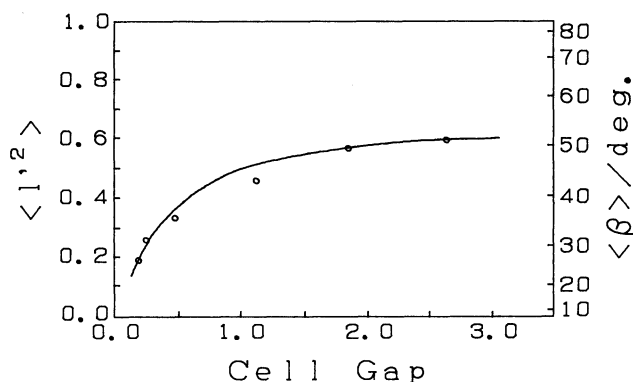


Fig. 6. Cell-gap dependence of the mean square of the direction cosine of the molecular orientation axis (OA) with respect to the x -axis $\langle l^2 \rangle$ and that of the mean angle $\langle \beta \rangle$ made by OA and the cell plane. The cell-gap dependences of $\langle l^2 \rangle$ and $\langle \beta \rangle$ are roughly estimated in the cell-gap range wider than that in Fig. 4; this is the reason why the number of the measured points in Fig. 6 is much smaller than that in Fig. 4. The cell gap is graduated by the absorbance for the first (354 nm) band of BEAB in the isotropic phase.

smaller, supporting our orientation model⁶⁾ for the LC molecules in the cell quantitatively.

Estimation of the Thickness of the Interface Region. According to the discrete model described in the Theoretical section, the thickness of the interface region ($=p^f/2$) is estimated as follows. The r_{12}^f ($=\varepsilon_1^f/\varepsilon_2^f$) values can be obtained for any of the assumed values of p^f and for any set of the two sandwich-type cells listed in Table 2 of Ref. 6 by substitution of the R_{12} , p , and r_{12}^b values

observed for the two cells into Eq. 8 to yield the $\varepsilon_1^f/\varepsilon_2^b$ and $\varepsilon_2^f/\varepsilon_2^b$ values. If the constraint on r_{12}^f ($r_{12}^f > 1.69$) is satisfied by all the r_{12}^f values obtained for all the sets of two cells assuming a common value of p^f , this common value of p^f can be regarded as a correct measure for the thickness of the interface region. This common value of p^f is found to be 0.15 using the R_{12} and r_{12}^b values⁶⁾ observed at 48°C; thus the thickness of the interface region is estimated to be 0.075 in absorbance scale, i.e., about 0.02 μm .

The authors wish to express their thanks to Professor Kozo Kuchitsu, Nagaoka University of Technology, for his critical reading of the manuscript. The present work was partially supported by a Grant-in-Aid for Scientific Research No. 58540252 from the Ministry of Education, Science and Culture.

References

- 1) R. S. Porter, E. M. Barall, II, and J. F. Johnson, *J. Chem. Phys.*, **45**, 1452 (1966); W. Helfrich, *J. Chem. Phys.*, **50**, 100 (1969); R. Chang, *Mater. Res. Bull.*, **7**, 267 (1972).
- 2) W. Maier and A. Saupe, *Z. Naturforsch., A*, **13A**, 564 (1958); **14A**, 882 (1959); **15A**, 287 (1960); **16A**, 816 (1961).
- 3) H. Kelker and R. Hatz, "Handbook of Liquid Crystals," Verlag Chemie, Weinheim (1980), Chaps. 3, 6, and 10; S. Chandrasekhar and N. V. Madhusudana, *Appl. Spectrosc. Rev.*, **6**, 189 (1972); M. J. Stephen and J. P. Straley, *Rev. Mod. Phys.*, **46**, 617 (1974); M. Sukigara, *Hyomen*, **16**, 189 (1978); P. G. de Gennes, "The Physics of Liquid Crystals," Clarendon Press, Oxford (1975), Chap. 2; "Introduction to Liquid Crystals," ed by E. B. Priestley, P. J. Wojtowicz, and P. Sheng, Plenum Press, New York (1975), Chaps. 3 and 6; "Liquid Crystals and Ordered Fluids," ed by J. F. Johnson and R. S. Porter, Plenum Press, New York (1974), Vol. 2, pp. 85, 125.
- 4) W. Maier and A. Saupe, *Z. Phys. Chem. N. F.*, **6**, 327 (1956); A. Saupe, *Z. Naturforsch., A*, **18A**, 336 (1963); A. Saupe, *Mol. Cryst. Liq. Cryst.*, **16**, 87 (1972).
- 5) M. Mizuno, T. Shinoda, H. Mada, and S. Kobayashi, *Mol. Cryst. Liq. Cryst.*, **41**, 155 (1978); **56**, 111 (1979).
- 6) M. Kobayashi, T. Kasahara, K. Nakajima, K. Maruyama, and Y. Tanizaki, *Bull. Chem. Soc. Jpn.*, **57**, 2695 (1984).
- 7) Y. Tanizaki, *Bull. Chem. Soc. Jpn.*, **32**, 75 (1959); **38**, 1798 (1965).